J Nanopart Res (2010) 12:2349–2353
DOI 10.1007/s11051-010-9980-8

BRIEF COMMUNICATION

Anchoring alpha-manganese oxide nanocrystallites on multi-walled carbon nanotubes as electrode materials for supercapacitor

Li Li · Zong-Yi Qin · Ling-Feng Wang · Hong-Jin Liu · Mei-Fang Zhu

Received: 22 October 2009 / Accepted: 28 May 2010 / Published online: 11 June 2010

Abstract The partial coverage of manganese oxide (MnO_2) particles was achieved on the surfaces of multi-walled carbon nanotubes (MWCNTs) through a facile hydrothermal process. These particles were demonstrated to be alpha-manganese dioxide (α-MnO_2) nanocrystallites, and exhibited the appearance of the whisker-shaped crystals with the length of 80–100 nm. In such a configuration, the uncovered CNTs in the nanocomposite acted as a good conductive pathway and the whisker-shaped MnO_2 nanocrystallites efficiently increased the contact of the electrolyte with the active materials. Thus, the highest specific capacitance of 550 F g^{-1} was achieved using the resulting nanocomposites as the supercapacitor electrode. In addition, the enhancement of the capacity retention was observed, with the nanocomposite losing only 10% of the maximum capacity after 1,500 cycles.

Keywords Manganese oxide · Carbon nanotube · Hydrothermal synthesis · Nanocomposite · Supercapacitor

L. Li · Z.-Y. Qin (✉) · L.-F. Wang · H.-J. Liu · M.-F. Zhu
State Key Laboratory for Modification of Chemical Fibers and Polymer Materials, College of Materials Science and Engineering, Donghua University, Shanghai 201620, People's Republic of China
e-mail: phqin@dhu.edu.cn

Introduction

The use of manganese oxides (MnO_2) for electrochemical energy storage has continued to expand to new applications, most recently to the field of electrochemical capacitors (Chou et al. 2008; Devaraj and Munichandraiah 2008; Estaline Amitha et al. 2009; Pang et al. 2000). The increasing worldwide interest in this area is based primarily on the anticipation that MnO_2 will ultimately serve as a low-cost alternative to disordered hydrous RuO_2 which provides extremely high specific capacitance as high as 760 F g^{-1}; however, it has several drawbacks, such as its being relatively expensive and toxic, that limit its commercialization of supercapacitors employing this material. MnO_2 appears to be a promising electrode material for supercapacitors, because of its high theoretical capacitance capacity in the range 1,100–1,300 F g^{-1} coupled with the low cost and environmental-friendly nature (Ma et al. 2004; Pang et al. 2000; Toupin et al. 2004; Xu et al. 2009).

Several groups have reported that, when MnO_2 is formed as the thin film with tens of nanometers thickness on planar current collector, anomalously high gravimetric capacitances ($\sim$700–1,380 F g^{-1}) can be observed (Ma et al. 2004; Pang et al. 2000; Toupin et al. 2004). Maintaining the MnO_2 thin film at the nanometer scale or coating in close proximity to the current collector could overcome the limitation of the poor electronic conductivity of MnO_2 (10^{-5}–10^{-6} Ω^{-1} cm^{-1}), and also reduce the distances for

the solid-state transport of insertion cations (Toupin et al. 2004). Therefore, it is very important to develop a facile and effective method to achieve high usability and dispersibility of MnO_2 in the composites. One effective solution is combining the properties of MnO_2 and carbon nanotubes (CNTs) with large surface area and low resistance to enhance to performance of the electrodes. Because the pseudocapacitive reaction of MnO_2 is a surface reaction, MnO_2/CNTs composites with MnO_2 thin film at the nanometer scale have been demonstrated to offer high specific capacity and good high-rate capability (Chen et al. 2007; Fan et al. 2006, 2008; Ma et al. 2008; Xie and Gao 2007).

In this study, the partial coverage of the low-dimensional crystallites of MnO_2 on the surfaces of multi-walled carbon nanotubes (MWCNTs) was prepared through a facile hydrothermal process. In such a configuration, it is expected that the uncovered CNTs in the nanocomposite could act as an efficient conductive pathway, the covered CNTs could serve as a high effective current collector and a substrate for the MnO_2, and the low-dimensional crystallites of MnO_2 with large surface area could efficiently increase the contact of the electrolyte with the active materials, thus making such nanocomposites with unique microstructure very promising for electrode materials for supercapacitor.

Experimental section

Commercial MWCNTs (purity $\geq$ 95 wt%, 20–40 nm in diameter, 5–15 μm in length, CVD method, Shenzhen Nanoharbor Co.) were added in saturated potassium permanganate solution, and the resultant suspensions were subsequently adjusted with hydrochloric acid until the pH decreased to around 1. After treating under low power ultrasonic irradiation for 6 h at 70 °C, the mixture was transferred to hydrothermal kettle, and allowed to dwell in the oven for 6 h under 140 °C. The system was then naturally cooled down to room temperature when the reaction was finished. The obtained product was filtered, washed thoroughly with deionized water to remove the remaining ions until the pH reached to 7, and then dried in a vacuum at 100 °C.

The morphology and microstructure of the resulting nanocomposites were characterized by a S-4800 (Hitachi) field emission scanning electron microscopy (SEM) , H-800 (Hitachi) transmission electron microscopy (TEM), and JEM-2010 (JEOL) high resolution SEM. The chemical composition was analyzed by energy dispersive spectroscopy (EDS) attached to SEM, and the crystal structure was determined on a RIGAKU D/Max-2550 PC X-ray diffraction instrument. The specific surface area (BET method) was determined by nitrogen adsorption–desorption isotherms using Quantachrome NOVA-2000 sorption analyzer.

Electrodes for supercapacitor were prepared by pressing the resulting nanocomposites into the nickel mash current collector under 5 MP and 100 °C for 30 min. The cyclic voltammogram was recorded on a CHI 1000A electrochemical working station (CH Instrument, Inc.) in 1 M Na_2SO_4 aqueous solution using a Pt wire as the counter electrode and Ag/AgCl as the reference electrode. All electrochemical experiments were carried out at room temperature. The specific capacitance obtained from the current–voltage curves could be calculated according to the following equation: $C = i/sm$, where 'i' was the average current, 's' was the potential sweep rate, and 'm' was the mass of each electrode.

Results and discussion

Figure 1a clearly shows that the partial coverage of the MnO_2 particles was successively achieved on the surfaces of MWCNTs during the hydrothermal process. It is found that the MWCNTs pretreated in saturated potassium permanganate solution remained in long tubes, while some long exposed tubes and tube ends can also be observed, which would lead to the decrease in the electrical resistivity of the nanocomposite. Figure 1b shows further that the MnO_2 particles on the surface of CNTs formed whisker-like microstructures with the length of 80–100 nm. Furthermore, the selected area electron diffraction pattern for whisker-shaped MnO_2 particles displayed only two diffraction rings as shown in Fig. 1c, which indicated the existence of the nanocrystalline microstructure of MnO_2. The chemical composition for the nanocomposites were further characterized using EDS attached to the SEM, which revealed that the nanocomposites contain the elements manganese, carbon, oxygen, and less than

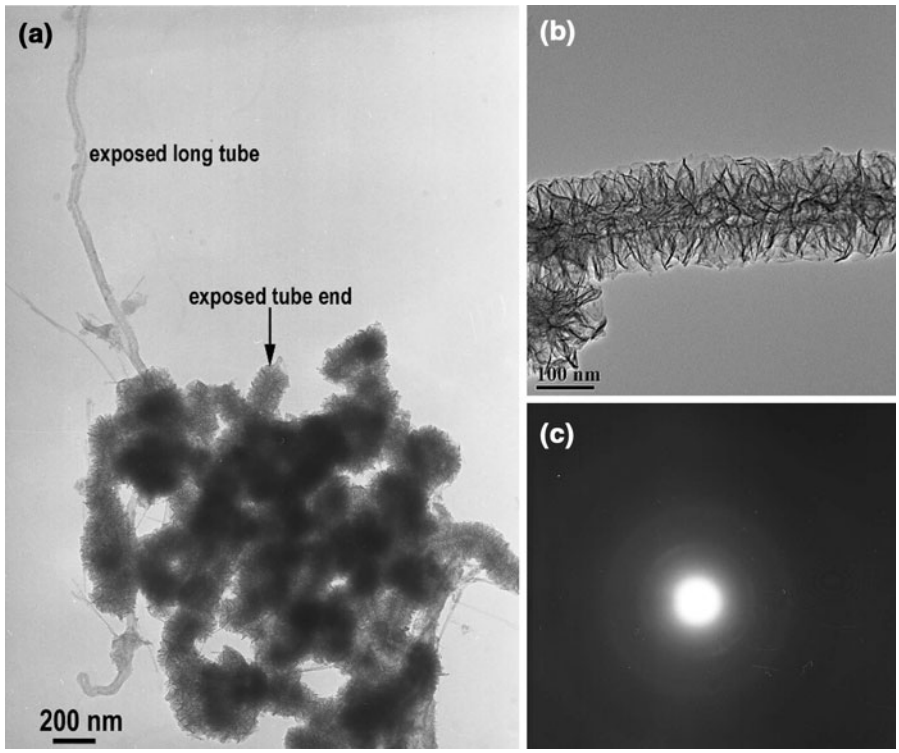

Fig. 1 Typical TEM images of MnO_2/MWCNTs (**a**) and (**b**) at different magnification, and the corresponding ED pattern (**c**)

8% wt/wt potassium probably located within the tunnel of MnO_2 nanocrystallites (Chen et al. 2007).

It is well known that the CNTs dispersed in an aqueous solution containing MnO_4^- ions can act as a reducing agent as well as a substrate for MnO_4^- ions, and promote the reduction process (Ma et al. 2007; Xie and Gao 2007). It is reasonably believed that the oxygen-containing functional groups can act as nucleation centers for the growth of MnO_2 nanocrystallites. During hydrothermal process, the MnO_4^- in the solution were first deoxidized to Mn^{2+} which were then adsorbed to the surfaces of the MWCNTs with oxygen-containing functional groups, such as carboxyl groups, through electrostatic attraction, and it in situ oxidized to low-dimensional MnO_2 nanocrystallites (Xie and Gao 2007). Interestingly, it is found that the partial coverage of whisker-shaped MnO_2 nanocrystallites was achieved on the surfaces of the MWCNTs treated the acidic solution of potassium permanganate under ultrasonic irradiation, and almost no MnO_2 nanocrystallites could be grown on the perfect surfaces of the MWCNTs (Fan et al. 2010), which provided an evidence supporting that the oxygen-containing functional groups could act as nucleating centers to grow the MnO_2 nanocrystallites. Although whisker-shaped α-MnO_2 nanocrystallites possess high aspect ratio and high surface area, which can contribute to the increase of the interface area between the active material and electrolyte, it is shown that the BET surface area is slightly increased from 52.772 $m^2\ g^{-1}$ for MWCNTs to 55.591 $m^2\ g^{-1}$ for the resulting nanocomposites.

X-ray diffraction patterns of the MWCNTs and the resulting nanocomposites are shown in the Fig. 2. The four weak, broad peaks situated at 2θ values of approximately 11.77°, 25.54°, 36.88°, and 65.5° can be attributed to the (110), (220), (400), and (002) diffraction of the α-MnO_2 (Ma et al. 2007; Subramanian et al. 2005; Xu et al. 2007), respectively. It is noted that the (110) plane for the composite diffracted at 11.77° has an interplanar distance of 7.51 angstroms; however, following the JCPDS card, the (110) plane has interplanar distance of 6.92 angstroms. The difference between the theoretical and the experimental results may be related to the small size of the MnO_2 particles. It is known that nanometer-sized materials have greater interplanar distance than the bulk ones. In addition, the absence of peaks with high diffraction intensities (such as (200) and (310)) together to the presence of others

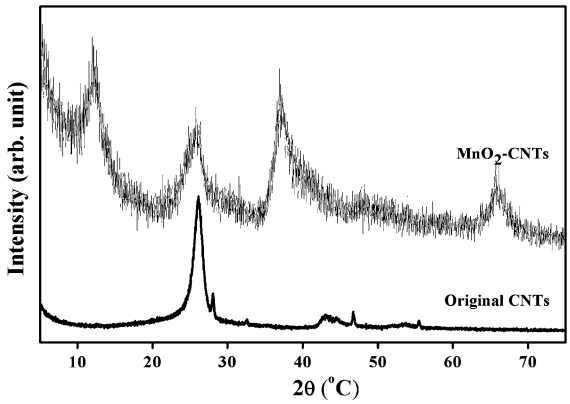

Fig. 2 The XRD patterns of the MWCNTs and MnO_2/MWCNTs nanocomposite

crystalline peaks in the XRD diffractogram illustrated in Fig. 2 is an indicative which amorphous and α-MnO_2 particles coexist in the composite. The capacitance properties are due to intercalation/deintercalation of protons or cations in MnO_2, thus the large 200 × 2 tunnels existing in the crystalline lattice of α-MnO_2 are expected to be very useful for capacitance studies (Devaraj and Munichandraiah 2008; Xu et al. 2007). In addition, four weak peaks located at 2θ values of approximately 26.5°, 42.4°, 54.7°, and 77.4° are characteristic of graphite in MWCNTs, corresponding to the (002), (100), (004), and (110) reflection planes, respectively (Xie and Gao 2007).

The supercapacitive properties of the resulting nanocomposites were evaluated by cyclic voltammetry at the scan rate of 2, 5 and 10 mV s^{-1}, respectively. Figure 3 shows clearly the rectangular and symmetric current–voltage characteristics of the excellent supercapacitor. Moreover, with the increase of the scan rate, current–voltage curves were still symmetric, indicating stable charge–discharge characteristics at high scan rate. The corresponding specific capacitance at the scan rate of 2, 5, and 10 mV s^{-1} were calculated to be 555, 550, and 480 F g^{-1}, respectively. The excellent supercapacitive properties of the resulting nanocomposites can be attributed to their unique microstructure. It is well known that the values of capacitance are strictly connected with the nature and surface of the electrode/electrolyte interface. On the one hand, the anchoring of whisker-shaped α-MnO_2 nanocrystallites on surface of MWCNTs can obviously increase the effective contact of the electrolyte and the active materials. On the other hand, CNTs in the nanocomposite can provide highly effective conductive pathway to provide more effective electrical transport from the active materials to the current collector.

Figure 4 shows the influence of the cycle numbers on the current–voltage curves at the scan rate of 5 mV s^{-1}. The capacitance loss of the resulting nanocomposites after 1,500 consecutive cycles is less than 10% and then maintaining stable, which can be attributed to the good electrochemical stability of the electrode. The improvement in the performance of the electrode benefits from the stable microstructure through anchoring whisker-shaped MnO_2 nanocrystallites onto the surface of MWCNTs and the presence of facile transport pathways in the

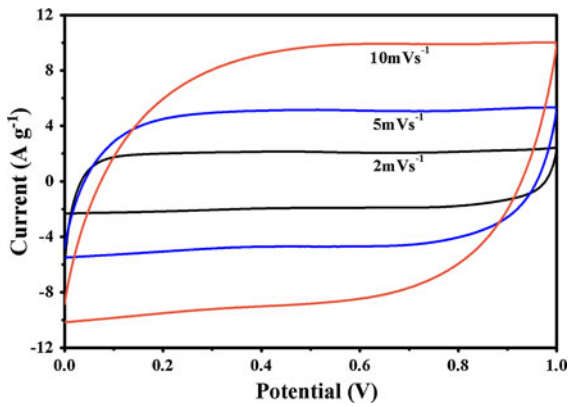

Fig. 3 The current–voltage curve of the MnO_2/MWCNTs nanocomposite at various scan rates

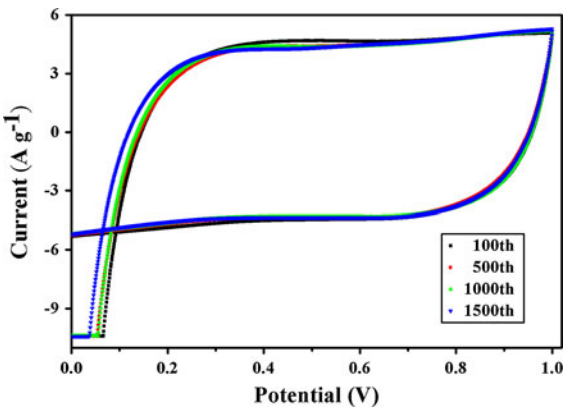

Fig. 4 The current–voltage curve of the MnO_2/MWCNTs nanocomposite as a function of the cycle number

nanocomposites. The long-term stability further proves that the resulting nanocomposite is a good candidate as a material for supercapacitor electrodes.

Conclusions

In this study, alpha-manganese dioxide nanocrystallites anchored on MWCNTs were achieved through a facile hydrothermal reaction route. The highest specific capacitance of 550 F g^{-1} at the scan rate of 2 mV s^{-1} was obtained by using such nanocomposites as supercapacitor electrode, and moreover the enhancement of the capacity retention was observed, just losing 10% of the maximum capacity after 1,500 cycles and then maintaining stable. The excellent supercapacitive properties of the resulting nanocomposites were attributed to their unique microstructure and a large tunnel cavity in the α-MnO_2 crystal structure, in which the uncovered MWCNTs in the nanocomposites acted as a good conductive pathway to facilitate electron transport from the active materials to the current collector, and the whisker-shaped α-MnO_2 nanocrystallites with large surface area could obviously increase the effective contact of the electrolyte and the active materials. Such nanocomposites with unique microstructure have been demonstrated to be excellent candidate electrode materials for high-performance supercapacitors.

Acknowledgment We gratefully acknowledge financial support from the Shanghai Pujiang Program (07PJ14005).

References

Chen Y, Liu CG, Liu C, Lu GQ, Cheng HM (2007) Growth of single-crystal α-MnO_2 nanorods on multi-walled carbon nanotubes. Mater Res Bull 42:1935–1941. doi:10.1016/j.materresbull.2006.12.005

Chou SL, Wang JZ, Chew SY, Liu HK, Dou SX (2008) Electrodeposition of MnO_2 nanowires on carbon nanotube paper as free-standing, flexible electrode for supercapacitors. Electrochem Commun 10:1724–1727. doi:10.1016/j.elecom.2008.08.051.7

Devaraj S, Munichandraiah N (2008) Effect of crystallographic structure of MnO_2 on its electrochemical capacitance properties. J Phys Chem C 112:4406–4417. doi:10.1021/jp7108785

Estaline Amitha F, Leela Mohana Reddy A, Ramaprabhu S (2009) A non-aqueous electrolyte-based asymmetric supercapacitor with polymer and metal oxide/multiwalled carbon nanotube electrodes. J Nanopart Res 11:725–729. doi:10.1007/s11051-008-9497-6

Fan Z, Chen JH, Wang MY, Cui KZ, Zhou HH, Kuang YF (2006) Preparation and characterization of manganese oxide/CNT composites as supercapacitive materials. Diam Relat Mater 15:1478–1483. doi:10.1016/j.diamond.2005.11.009

Fan Z, Chen JH, Zhang B, Liu B, Zhong XX, Kuang YF (2008) High dispersion of γ-MnO_2 on well-aligned carbon nanotube arrays and its application in supercapacitors. Diam Relat Mater 17:1943–1948. doi:10.1016/j.diamond.2008.04.015

Fan QQ, Qin ZY, Liang X, Li L, Wu WH, Zhu MF (2010) Reducing defects on multi-walled carbon nanotube surfaces induced by low-power ultrasonic assisted hydrochloric acid treatment. J Exp Nanosci (in press). doi:10.1080/17458080903536541

Ma R, Bando Y, Zhang L, Sasaki T (2004) Layered MnO_2 nanobelts: hydrothermal synthesis and electrochemical measurements. Adv Mater 16:918–922. doi:10.1002/adma.200306592

Ma SB, Ahn KY, Lee ES, Oh KH, Kim KB (2007) Synthesis and characterization of manganese dioxide spontaneously coated on carbon nanotubes. Carbon 45:375–382. doi:10.1016/j.carbon.2006.09.006

Ma SB, Nam KW, Yoon WS, Yang XQ, Ahn KY, Oh KH, Kim KB (2008) Electrochemical properties of manganese oxide coated onto carbon nanotubes for energy-storage applications. J Power Sour 178:483–489. doi:10.1016/j.jpowsour.2007.12.027

Pang SC, Anderson MA, Chapman TW (2000) Novel electrode materials for thin-film ultracapacitors: comparison of electrochemical properties of sol-gel-derived and electrodeposited manganese dioxide. J Electrochem Soc 147:444–450. doi:S0013-4651(99)04-063-X

Subramanian V, Zhu H, Vajtai R, Ajayan P, Wei B (2005) Hydrothermal synthesis and pseudocapacitance properties of MnO_2 nanostructures. J Phys Chem B 109:20207–20214. doi:10.1021/jp0543330

Toupin M, Brousse T, Belanger D (2004) Charge storage mechanism of MnO_2 electrode used in aqueous electrochemical capacitor. Chem Mater 16:3184–3190. doi:10.1021/cm049649j

Xie X, Gao L (2007) Characterization of a manganese dioxide/carbon nanotube composite fabricated using an in situ coating method. Carbon 45:2365–2373. doi:10.1016/j.carbon.2007.07.014

Xu M, Kong L, Zhou W, Li H (2007) Hydrothermal synthesis and pseudocapacitance properties of α-MnO_2 hollow spheres and hollow urchins. J Phys Chem C 111:19141–19147. doi:10.1021/jp076730b

Xu N, Liu ZH, Ma X, Qiao S, Yuan J (2009) Controlled synthesis and characterization of layered manganese oxide nanostructures with different morphologies. J Nanopart Res 11:1107–1115. doi:10.1007/s11051-008-9517-6